Article:
Zia, Q, Tabassum, M, Lu, Z et al. (6 more authors) (2020) Porous poly(L–lactic acid)/chitosan nanofibres for copper ion adsorption. Carbohydrate Polymers, 227. 115343. ISSN 0144-8617

https://doi.org/10.1016/j.carbpol.2019.115343

Porous poly(L–lactic acid)/chitosan nanofibres for copper ion adsorption

Qasim Zia[a], Madeeha Tabassum[b], Zihan Lu[a], Muhammad Tauseef Khawar[a], Jun Song[a], Hugh Gong[a], Jinmin Meng[a], Zhi Li[c] and Jiashen Li[*a]

[a]Department of Materials, The University of Manchester, Manchester M13 9PL, United Kingdom.

[b]School of Engineering & Materials Science, Queen Mary University of London, Mile End Road E1 4NS, United Kingdom.

[c]College of Textile and Garment, Southwest University, Chongqing 400715, China.

[*]Corresponding Author: Jiashen Li

Email: Jiashen.li@manchester.ac.uk

Abstract

Porous poly(L-lactic acid) (PLLA) nanofibrous membrane with the high surface area was developed by electrospinning and post acetone treatment and used as a substrate for deposition of chitosan. Chitosan was coated onto porous nanofibrous membrane via direct immersion coating method. The porous PLLA/chitosan structure provided chitosan a high surface framework to fully and effectively adsorb heavy metal ions from water and showed higher and faster ion adsorption. The composite membrane was used to eliminate copper ions from aqueous solutions. Chitosan acts as an adsorbent due to the presence of aminic and hydroxide groups which are operating sites for the capture of copper ions. The maximum adsorption capacity of copper ions reached 111.66±3.22 mg/g at pH (7), interaction time (10 min) and temperature (25 °C). The adsorption kinetics of copper ions was established and was well agreed with the second-order model and Langmuir isotherm. Finally, the thermodynamic parameters were studied.

Keywords: Chitosan, Porous PLLA nanofibres, Adsorption, Langmuir model

1. Introduction

The ground and industrial wastewater contain several contaminations including heavy metal ions, for instance, Cu, Pb, Ni, As, Cr, Hg, and Cd. The rise in the amount of heavy metal in the groundwater is due to contamination by many industries including paper, battery, refineries, metallurgy, leather and textile **(Lalita, Singh, & Sharma, 2017)**. The European Commission Science for Environment Policy (SEP) **(Unit, 2013)** has stated heavy metals as most common contaminants (31%) in the groundwater second to the mineral oil (22%). It is important to remove these elements as their presence acts as a severe threat to human well-being and ecosystem because of their toxic effects **(Tirtom, Dinçer, Becerik, Aydemir, & Çelik, 2012; Wan, Kan, Rogel, & Dalida, 2010; Zhang et al., 2008; Zhao, Repo, Yin, & Sillanpaa, 2013)**. Among heavy metals, copper (Cu) is one of the most commonly used elements in the production industries such as electrical, antifouling and paint industries. It has many toxic effects on human health including cancer, liver damage, Wilson disease, and insomnia **(Barakat, 2011; Keizer, 2001)**. The protection agency for the environment (USA) has fixed the highest contamination limit of copper ions in the water to 0.25 mg/L. Beyond this value, it causes severe effects on health including cancer, organ damage, nervous system damage and in extreme cases death **(Barakat, 2011; Kurniawan, Chan, Lo, & Babel, 2006)**. Multiple techniques are in practice with varying efficiencies to remove the Cu ions from water, including chemical precipitation, membrane filtration, adsorption, photocatalysis, ion exchange and reverse osmosis **(Acosta,**

Rodríguez, Gutiérrez, & Moctezuma, 2004; Dubey & Gopal, 2007). However, each of these techniques has certain limitations. For example, chemical precipitation generates a large amount of sludge (**Kurniawan et al., 2006**). Membrane filtration and reverse osmosis require high operational costs (**Kurniawan et al., 2006**), while photocatalysis is a relatively slow process (**Barakat, Chen, & Huang, 2004**). Out of these methods, ion adsorption is one of the most practical methods for water filtration due to its cost-effectiveness, high binding capacities, and facile operation (**Aklil, Mouflih, & Sebti, 2004**). Nanoporous glass, sand, palm oil, chitosan and ceramic alumina are used for the adsorption of heavy metals from the water (**Bassi, Prasher, & Simpson, 2000; Boddu, Abburi, Talbott, Smith, & Haasch, 2008; Liu, Tokura, Haruki, Nishi, & Sakairi, 2002; Moussavi & Khosravi, 2010; Wan et al., 2010**).

Chitosan is another suitable material for the removal of heavy metals as it contains active amino and hydroxyl groups on its surface. These groups act as anchors to capture and fix metal ions from water. The higher density of active sites chitosan has, the more and faster it adsorbs ions. Moreover, it is easily available, biodegradable, non-toxic and biocompatible. The **Figure S1** displays the chemical structure of chitosan (**Habiba, Siddique, Joo, et al., 2017; Habiba, Siddique, Talebian, et al., 2017; Mututuvari & Tran, 2014; Salehi, Daraei, & Arabi Shamsabadi, 2016; Shen, Wang, Xu, & Luo, 2013**).

The large scale application of chitosan in adsorption of heavy metals ions is limited by its low mechanical strength, pH sensitivity, swelling, and low surface area (**Cooper, Oldinski, Ma, Bryers, & Zhang, 2013; Premakshi, Ramesh, & Kariduraganavar, 2015; Seo et al., 2014**). The properties of chitosan can be improved by crosslinking or immobilizing it on a support material. Previously the chitosan has been crosslinked with glutaraldehyde (**Chen, Yang, Chen, Chen, & Chen, 2009**), epichlorohydrin (**Chen, Liu, Chen, & Chen, 2008**), and diethylenetriaminepentacetic acid (**Bhatt, Sreedhar, & Padmaja, 2017**) to raise the mechanical strength and chemical balance. Whilst crosslinking improves the mechanical properties, it reduces the density of active sites which weakens the capacity of chitosan to purify water (**Zhang et al., 2008**). Coating of chitosan on a support material is another viable approach to improve its properties while keeping most of the functional groups on the exterior of chitosan (**Wan, Petrisor, Lai, Kim, & Yen, 2004**). Recently, Yaolin et al. (**Niu, Ying, Li, Wang, & Jia, 2017**) reported the removal of Cu(II), Pb(II) and Zn(II) ions by chitosan coated polyethylene terephthalate (PET) adsorbent. Franco et al. (**Ferrero, Tonetti, & Periolatto, 2014**) examined the adsorption of Cu(II) and Cr(VI) ions from water on chitosan-coated cotton gauze. Qu et al. (**R. Qu et al., 2009; Rongjun Qu et al., 2009; Zhang et al., 2008**) coated chitosan onto cotton fibre for the removal of Au(III), Hg(II), Cd(II), Cu(II) and Ni(II) ions from wastewater. It was observed in these studies that the substrate plays an important role in providing chitosan a stable framework for adsorption from water.

In the present study, we have used highly porous poly(L-lactic acid) (PLLA) nanoporous fibrous membrane as supporting material for chitosan. PLLA is a kind of biocompatible, biodegradable, eco-friendly and cost-effective material. These properties make it a suitable host material for water purification (**Neumann, Flores-Sahagun, & Ribeiro, 2017; Ying W, 2006).** PLLA fibres can be produced by electrospinning which is a straightforward, versatile and cost-effective technique and allows the control of fibre diameter from nanometer to micrometer (**Bhardwaj & Kundu, 2010; Dorati et al., 2018**). The electrospun nanofibres are considered to be the next generation material for water filtration because of large porosity, tunable orifice size and high surface area to volume ratio (**Habiba, Siddique, Talebian, et al., 2017; Huang, Zhang, Kotaki, & Ramakrishna, 2003**). The large surface area provided by electrospun fibres can enhance the ion adsorption capacity of

composite material. To utilize these properties, chitosan was coated on porous PLLA fibrous membrane by immersion method for preparation of a composite for water filtration (CHPLLA). Without further crosslinking, chitosan could keep most of its active sites for metal ion adsorption. The adsorption performance of CHPLLA for Cu (II) heavy metal from water was examined. The adsorption parameters, including effects of pH, initial metal concentration, temperature and chitosan quantity on the adsorption capability of CHPLLA for Cu (II) ions, the kinetics of adsorption, and isotherm models were explored and procedure for the adsorption of copper ions was discussed. To the best of our information, this is the first study of porous PLLA nanofibres as supportive materials for removal of Cu (II) ions from water.

2. Experimental

2.1.Materials

Chitosan with low molecular weight (M_w = 50,000-190,000 Da), 75-85 % deacetylated was purchased from Sigma Aldrich. Poly(L-lactic acid) (PLLA) (MW=1.43×10^6) was supplied by PURAC biochem, Holland. Dichloromethane (DCM, 99.99%) was purchased from Sigma Aldrich. Dimethylformamide (DMF, 99.8%), was purchased from Fisher Scientific Ltd. Ethanol (EtOH, 99.97%) and acetone (99.70%) were purchased from VWR Science Company., Limited. Deionized water was acquired from USF-ELGA water filter in the laboratory. Copper sulfate pentahydrate ($CuSO_4.5H_2O$) was purchased from Fisher Scientific Ltd.

2.2.Preparation of porous PLLA nanofibres

The porous PLLA nanofibres were prepared by electrospinning technique and subsequent solvent treatment. First, 1.8 wt % PLLA was dissolved in DCM and DMF with a 19:1 w/w by stirring and heating at 50 °C in the closed container to avoid the evaporation of solvents until the solution becomes transparent and PLLA was completely dissolved. The mixture was filled in a 30 ml syringe with a metal needle (19G) and fixed on an electrospinning setup. The distance between the needle tip and the metal collector (roller) was maintained to be 30 cm and 23 kV power source was used to charge the mixture. The mixture was released towards the revolving grounded roller (200 rpm) to collect nanofibrous membranes. The collected membranes were allowed to dry overnight. The produced fibrous membrane was immersed in acetone for 5 minutes at room temperature and then dried in the fume cupboard to get porous nanofibrous mats.

2.3.Coating of chitosan

The coating of chitosan onto porous PLLA nanofibres was achieved by a direct immersion coating method. For this, aqueous solutions of chitosan (0.5, 1, 2 and 3 wt%) with pH 3 were prepared by dissolving chitosan (0.1, 0.2, 0.4, 0.6 g) in 20 ml of 0.5 % (v/v) acetic acid solution by magnetically mixing at room temperature. Electrospun porous PLLA nanofibrous membranes were immersed in chitosan mixture for 10 mins, withdrawn from the solution, blotted carefully and dried to a constant mass.

2.4.Characterizations

The morphology of nanofibrous membranes was characterized by Quanta 250 FEG electron microscope (FE-SEM), USA. Elemental analysis was conducted using Energy Dispersive Spectrophotometer (EDS) by Oxford Instruments. Fourier transform infrared spectra (FTIR) was recorded on NICOLET 5700 spectrophotometer. X-Ray Diffraction (XRD) was performed using

PANalytical X'pert PRO USA. The quantification of heavy metals was done using Inductively coupled plasma-atomic emission spectroscopy (ICP-AES).

2.5. Adsorption experiments

The adsorption of copper ions on the chitosan modified porous PLLA nanofibres (CHPLLA) was observed with varying parameters of chitosan concentration (0.5-3 wt%), pH (3-10), interaction period (1-30 min), original Cu (II) ions quantity (50-200 mg/L) and temperature (25-50 °C) in a group structure. The amount of the porous PLLA nanofibres was changed in order to provide the same amount of adsorbent after coating with different chitosan concentrations (0.6 mg/20 mL). The original pH of the copper ion solutions was modified with HNO_3 (0.1 M) and NaOH (0.1 M). The adsorption ability (q_e) of copper ions was computed by following mathematical expression (1):

$$\mathbf{q_e} = \frac{(\mathbf{C_i} - \mathbf{C_e})\mathbf{V}}{\mathbf{M}} \quad (1)$$

Where C_i and C_e (mg/L) are initial and final concentrations of copper ions, respectively. V is the solution quantity (mL) and M is the mass of adsorbent (mg). The mathematical modelling of kinetic, isotherm and thermodynamic factors of adsorption was computed by regression equation using Origin software.

2.6. Swelling test of chitosan-coated PLLA nanofibers

The swelling behaviour of CHPLLA nanofibres was studied by adding 0.2 g of chitosan and 1 wt% CHPLLA nanofibres in each of distilled water, dilute acidic and alkaline solutions at room temperature for 12 hours. Chitosan and CHPLLA nanofibres were tested to compare the swelling behaviour in different environments. The percentage of swelling was calculated by using the following equation:

$$\textbf{Percentage of swelling} = \frac{\mathbf{W_s} - \mathbf{W_d}}{\mathbf{W_D}} \times \mathbf{100}\ \% \quad (2)$$

Where W_d and W_s is the weight of dry and swollen chitosan-coated PLLA nanofibres, respectively.

3. Results and Discussions

3.1. Characterization of chitosan-coated porous PLLA nanofibres

The FTIR spectra of CHPLLA nanofibres, chitosan, and porous PLLA nanofibres are demonstrated in **Figure 1 (a,b and c)**. The spectrum shows bands at 2919 and 3000 cm^{-1} for porous PLLA, 3000 cm^{-1} for CHPLLA and 2936, 2857 cm^{-1} for chitosan. These bands belong to C-H stretch from CH_3. The bands at 1741 cm^{-1} for both PLLA and CHPLLA corresponds to C═O extending of ester. C-O-C extending vibration was observed at 1082 and 1185 cm^{-1} in both PLLA and CHPLLA. In CHPLLA spectrum, bands at 1541 and 1511 cm^{-1} are assigned to N-H pattern of the chitosan as shown in **Figure 1(b) (Razzaz, Ghorban, Hosayni, Irani, & Aliabadi, 2016)**. The presence of these bands suggests that chitosan was successfully coated on porous PLLA nanofibres.

Figure 2 shows the FESEM images of porous PLLA nanofibres. The surface of the nanofibres is rough and the uniform porous network is observed on nanofibres. After electrospun PLLA fibres were treated by acetone, the fibres were changed to porous ones which provide chitosan a substrate with a very high surface area.

Figure 3 (a, b, c and d) exhibits FE-SEM images of porous CHPLLA nanofibres. The exterior of the nanofibres after chitosan coating is comparatively smooth. For 0.5 and 1 % of chitosan concentration, the formation of thin chitosan coating is observed on nanofibres while the porous structure is still visible. The coating becomes thicker and covers the porous structure of nanofibres for 2 and 3 % of chitosan.

XRD patterns of porous PLLA nanofibres, chitosan film, and CHPLLA nanofibres are displayed in **Figure S2**. Diffraction peaks of porous PLLA nanofibres at 2θ = 14.7°, 16.6°, and 19.01° are derived from 104, 200 and 203 phases of α phase **(Naga, Yoshida, Inui, Noguchi, & Murase, 2011)**. The results indicate that PLLA was crystallized as α phase after treatment with acetone. The diffractogram of chitosan consisted of two major peaks at 2θ = 10.9° and 20.7°**(Wang et al., 2016)**. Compared with chitosan and porous PLLA nanofibres, the diffractogram of chitosan modified porous PLLA nanofibres exhibited some changes in peak width and peak position. The peak at 14.7° shifted to the left and its width was decreased, while the peak at 16.6° shows a decrease in width. Such stronger and narrow peaks indicated a more crystalline phase of the CHPLLA. In addition, the peak at 10.9° of chitosan disappeared and a new crystalline peak of PLLA appeared at 12.3°, which was confirmed from ICDD card no. 00-064-1624. It implies that the CHPLLA was considerably more crystalline than porous PLLA nanofibres. Chitosan acted as a nucleating agent and caused the fast crystallization of PLLA as stated in previous studies **(Correlo et al., 2005; Râpă et al., 2016)**.

3.2.Adsorption of Cu ions on chitosan-coated porous PLLA nanofibres

Porous PLLA nanofibrous membrane is prepared, coated with chitosan and copper ions are adsorbed as exhibits in **Figure 4**. The presence of Cu ions was displayed by a clear blue colour of the CHPLLA nanofibres after the adsorption process **Figure 5**. Furthermore, the EDS spectra presented in **Figure S3 (a) and (b)** reveal the existence of Cu peaks in chitosan-coated porous PLLA nanofibres as compared to the uncoated porous PLLA nanofibres. Therefore, the results suggest that the chitosan active sites are capable to act as active sites for adsorption of copper ions.

.

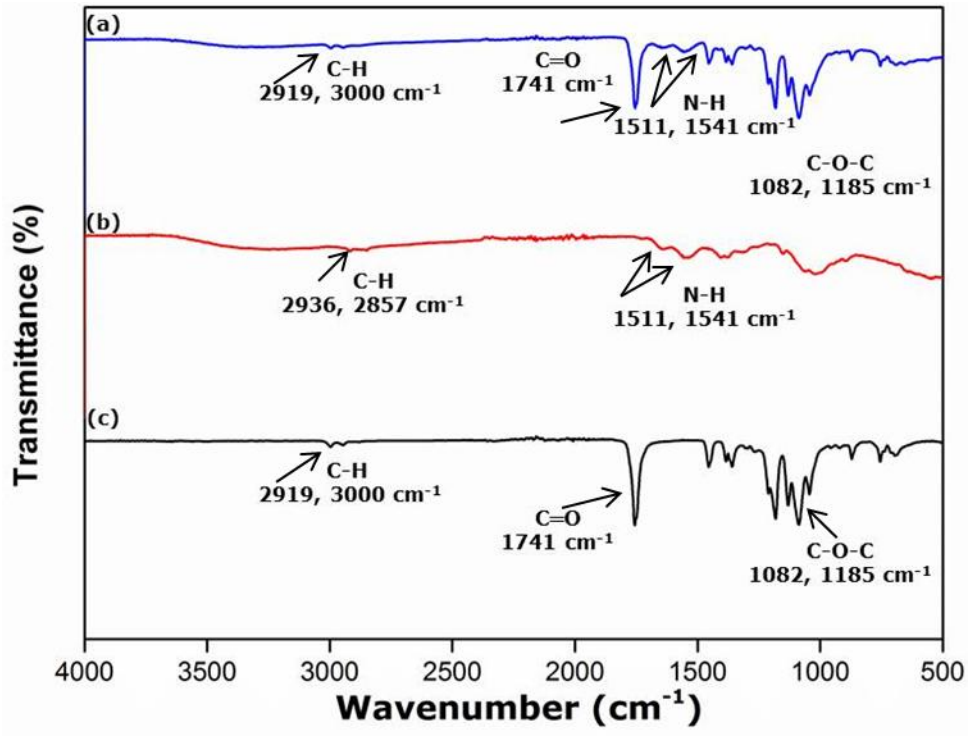

Figure 1. FTIR of (a): chitosan coated porous PLLA nanofibres (b): pure chitosan (c): porous PLLA nanofibres

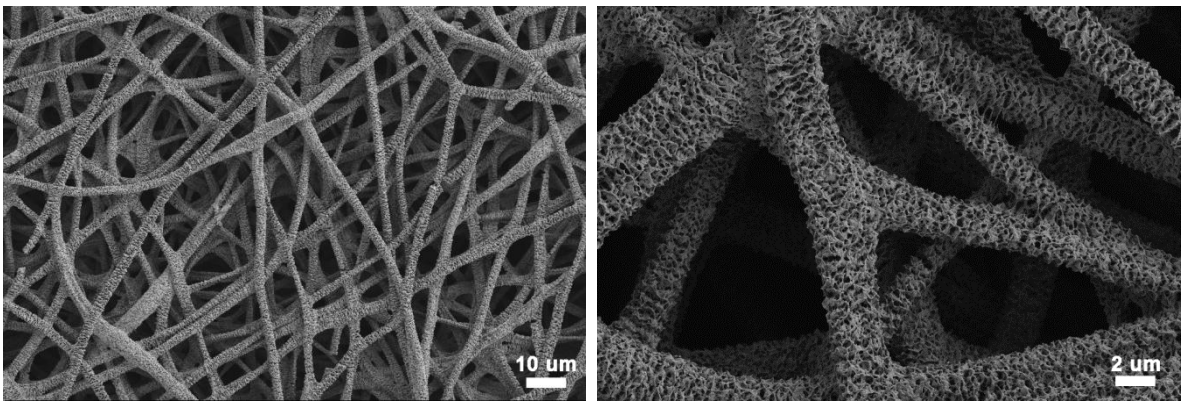

Figure 2. SEM of porous PLLA nanofibres with different magnifications.

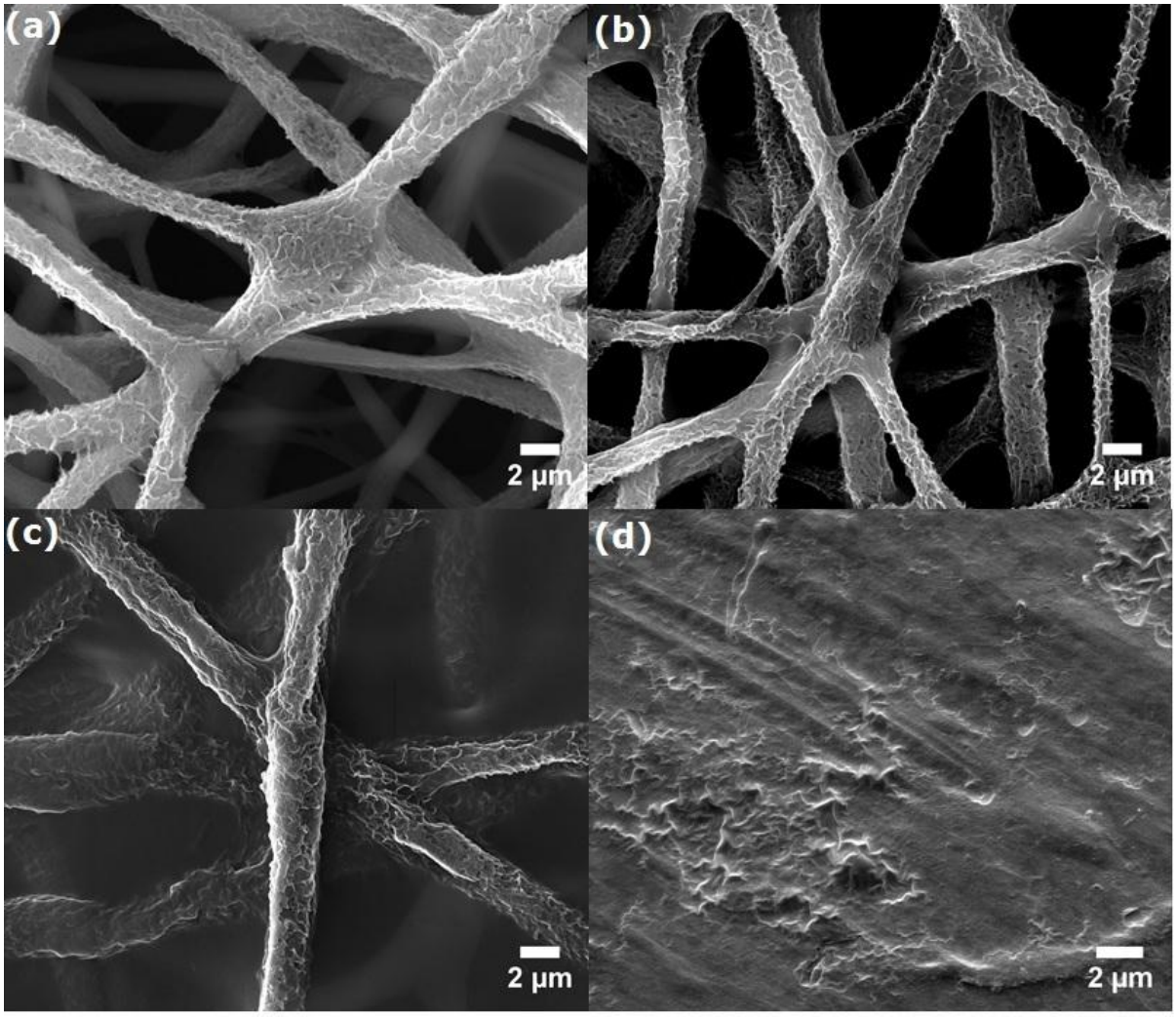

Figure 3. SEM of chitosan-coated porous PLLA nanofibres (a): 0.5% chitosan, (b): 1% chitosan (c): 2% chitosan & (d): 3% chitosan.

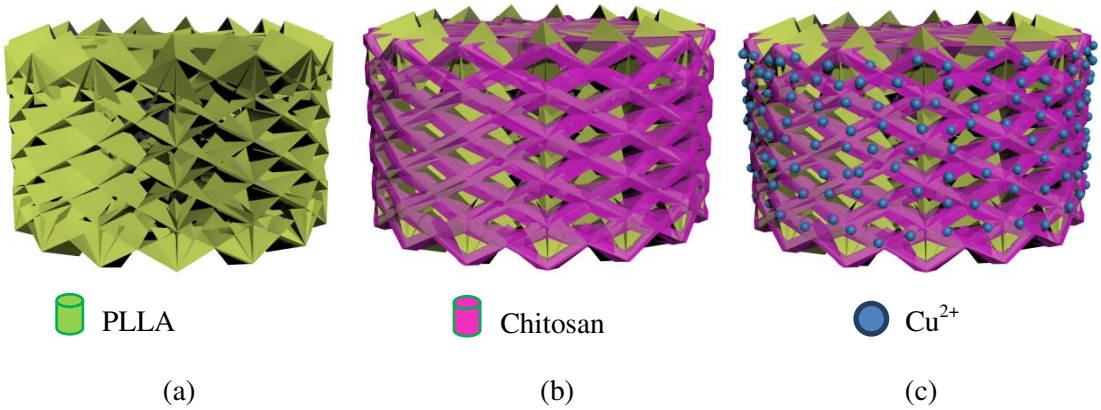

Figure 4. Schematic of experimental methodology: (a) porous PLLA fiber; (b) porous PLLA fiber with chitosan coating; (c) copper ions are adsorbed by chitosan.

Figure 5. The contrast between hue of chitosan-coated porous PLLA nanofibres without and with adsorption of Cu (II) ions.

3.3. Stability studies of chitosan-coated porous PLLA nanofibres

The swelling behaviour of chitosan and chitosan-coated porous PLLA nanofibres is shown in **Table S1**. It is known that chitosan is soluble in dilute acidic environments due to the protonation of amino groups in acidic media. The suitable evidence of chitosan coating on porous PLLA nanofibres is the less swelling of chitosan in dilute acetic acid, distilled water, and NaOH solution. This can be attributed to the strong adhesion of chitosan on porous PLLA nanofibres.

3.4.Impact of chitosan concentration on the adsorption capacity

To observe the impact of chitosan concentration on the exclusion of copper ions, the CHPLLA nanofibrous sorbents with varying concentrations (0.5, 1, 2 and 3 wt.%) were prepared. The performance of nanofibre adsorbents was evaluated at a copper initial quantity of 100 mg/L with a pH of 7, adsorbent mass of 0.6 mg/20 mL, the interaction time of 30 mins and a temperature of 25 °C. The results are displayed in **Figure 6(a)**. It is observed that Cu (II) adsorption increases by increasing the concentration of chitosan up to 1 %. It is expected that the thin film of chitosan formed up to 1 % concentration increases the active sites such as $–NH_3$ for the adsorption procedure. With an increase in the amount of chitosan beyond this point, the adsorption capability of copper ions decreased. This behavior could be credited to accumulation and thickening of chitosan at a higher concentration which decreased the surface area of nanofibres and reduced the available functional sites for copper ions adsorption. Therefore, the concentration of 1 % is considered as an optimal value for the coating of porous PLLA nanofibres with chitosan.

3.5.Impact of pH on adsorption capacity

The effect of solution pH on the surface reaction was studied by maintaining the number of copper ions to 100 mg/L, adsorbent amount to 0.6 mg/20 mL and contact time of 30 mins. The measurements were executed at room temperature in pH between 3-10. The findings are displayed in **Figure 6(b)**. An increasing trend of adsorption capacity is observed with increasing pH value and the maximum value is found at 7. After this limit, the adsorption capacity starts to decrease and this trend continues until 10. This behaviour can be explicated by the existence of the surplus amount of hydrogen ion at low pH which restricts the reaction of ions with $–NH_3$ working groups of chitosan. Moreover, chitosan is susceptible to dissolution in an acidic environment. Therefore, a maximum adsorption value was found in neutral conditions. At higher pH values, Cu (II) ions form hydroxide complexes

($Cu(OH)_2$) which caused a decrease in adsorption capacities of CHPLLA adsorbent. Based on these findings, pH 7 is designated as an optimal value for more adsorption studies.

3.6.Impact of temperature on adsorption capacity

The adsorption process of Cu (II) ions using fabricated CHPLLA nanofibrous adsorbent was conducted at temperatures of 25, 30, 40 and 50 °C, the concentration of 100 mg/L for copper ions, the adsorbent dosage of 0.6 mg/20 mL and the interaction time of 30 mins. The glass transition temperature of PLLA is reported at 65 °C in the previous literature **(Middleton & Tipton, 2000)**. Therefore, temperatures up to 50 °C will not affect the mechanical integrity of the porous PLLA membrane. **Figure 6(c)** shows the impact of temperature on the adsorption strength of copper ions. It is observed that adsorption capability decreases with increasing temperature. At high temperature, the thickness of the surface layer decreases as copper ions start to leave the adsorbent surface and go into the solution. This led to the decline in adsorption of copper (II) ions at elevated temperature **(Aksu & Kutsal, 1991)**. The decrease in adsorption capability with rising temperature suggests weak adsorption synergy between the adsorbent surface and the metal ion, which refers to physisorption. Therefore, 25 °C is considered as the ideal temperature for more studies of adsorption.

3.7.Kinetics of adsorption

Figure 6(d) illustrates the adsorption ability as a function of time from 1-30 mins CHPLLA porous adsorbent in 20 mL of individual changed copper concentration. Initially, the rate of copper removal was fast due to a large amount of available active sites on the adsorbent surface and became constant after that. This is due to the reason that all the adsorption positions were occupied by adsorbed metals **(Labidi, Salaberria, Fernandes, Labidi, & Abderrabba, 2016)**. It is notable that within only 10 minutes of interaction time maximum elimination of copper ions was attained. The **Figure 6(d)** also illustrates that the adsorption rate of copper ions was reliant on the primary quantity of copper ions as witnessed in a previous study **(Nagib, Inoue, Yamaguchi, & Tamaru, 1999)**. As presented, the adsorption capability of CHPLLA adsorbent was increased for larger copper ions initial quantity. This observation can be credited to the fact that the transfer of mass effect and driving force of concentration gradient are directly proportional to the initial quantity of metal ions **(Wan et al., 2010)**.

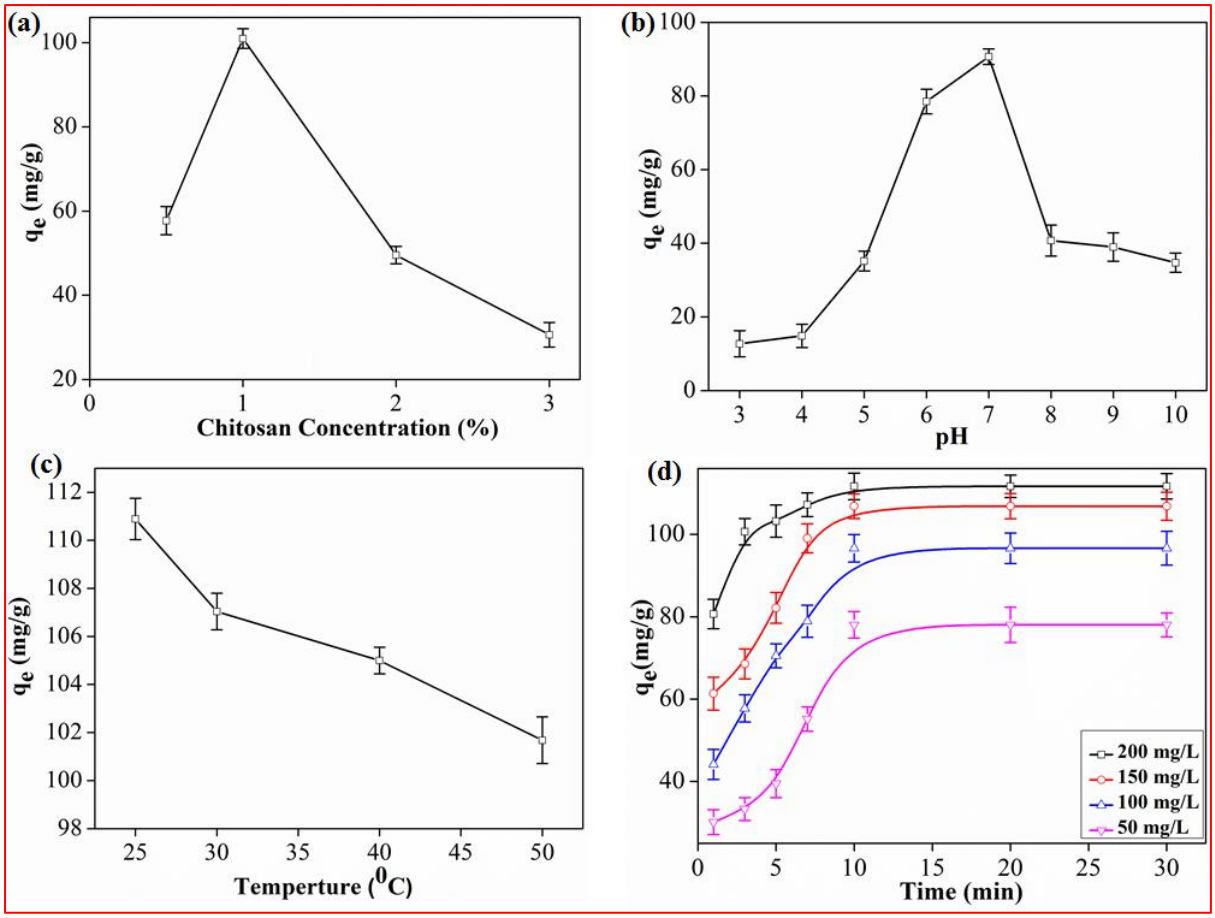

Figure 6. Experimental conditions of adsorption (a): effect of chitosan concentration, (b): effect of pH, (c): effect of temperature, (d): adsorption kinetics.

3.8.Mathematical modelling of adsorption kinetics

To study the time of adsorption as well as the time defining the stage of the adsorption process, first-order and second-order kinetic models were studied to simulate the adsorption experimental numbers. Widely used first-order kinetic model for absorption in the solid/liquid complex is indicated as **(Chiou & Li, 2003)**:

$$\log(q_{equ} - q_{time}) = \log(q_{equ}) - \frac{k_1}{2.303}t \quad (3)$$

Pseudo-second order model is expressed as follows:

$$\frac{t}{q_{time}} = \frac{1}{k_2 q_{equ}^2} + \frac{1}{q_{equ}}t \quad (4)$$

Where q_{time} (mg/g) and q_{equ} (mg/g) are the quantities of metals adsorbed at the time (t) and at equilibrium respectively. While k_1 (min^{-1}) and k_2 (mg/g min^{-1}) are the constants of first and second-order reaction models.

Figure 7(a) and **Table 1** indicates that the first-order model did not apt the adsorption investigated statistics well. The correlation coefficients R^2 for the theoretical values of equilibrium adsorption capacity (q_e) is very low because first order is only appropriate for explaining the numbers that are

near to the equilibrium adsorption **(Plazinski, Rudzinski, & Plazinska, 2009)**. As shown in **Figure 7(b)** and **Table 1**, pseudo-second-order model describes the adsorption system well since the experimental adsorption values are close to the calculated ones, and the R^2 values are greater than 0.999, demonstrating that the adsorption procedure is administered by the surface reaction **(Repo, Warchoł, Bhatnagar, & Sillanpää, 2011)**.

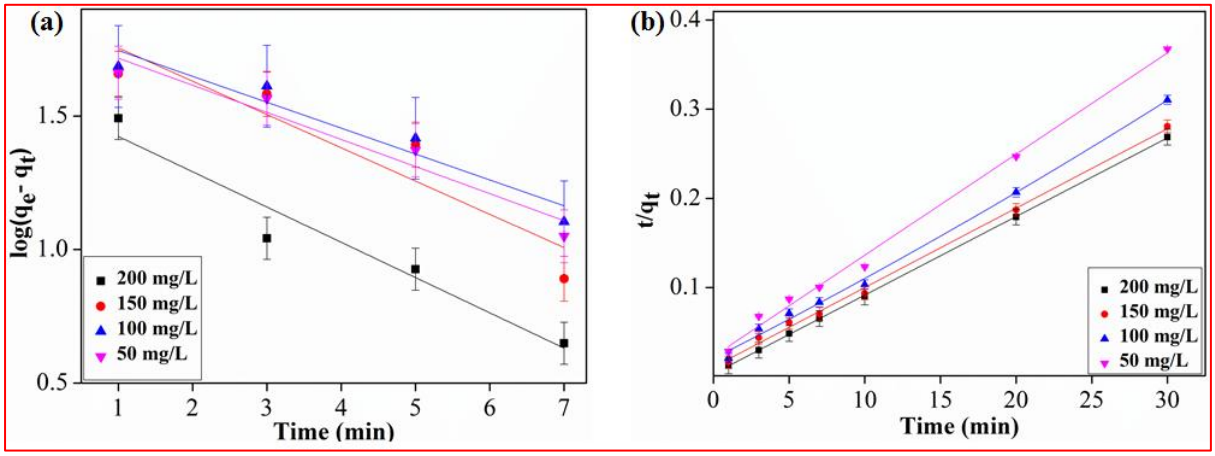

Figure 7. (a): pseudo-first-order reaction kinetics, (b): pseudo-second reaction kinetics.

Table 1 Parameters of Pseudo first and second-order reaction kinetics

Concentration (mg/L)	First-order kinetics			Second-order kinetics				
	k_1 (min^{-1})	R^2	SD	k_2 (g mg^{-1} min^{-1})	$q_{equ, exp}$ (mg g^{-1})	$q_{equ, cal}$ (mg g^{-1})	SD	R^2
50	0.0440	0.94	±0.079	0.00568	81.04	88.10	±0.0089	0.99
100	0.0420	0.92	±0.084	0.00577	96.64	103.30	±0.0071	0.99
150	0.0540	0.86	±0.153	0.00735	106.84	112.23	±0.0052	0.99
200	0.0573	0.94	±0.099	0.0237	111.66	113.37	±0.001	0.99

3.9.Modelling of adsorption isotherms

Isotherm models are studied to make a model of adsorption capability of adsorbents against the amount of adsorbate at equilibrium conditions. In this study, we have used the Langmuir model and the Freundlich model to study the adsorption process.

The Langmuir model considered that there are a constant amount of adsorption locations present on the adsorbent surface, active sites are of equal size and shape on a solid surface and each vacant site can bind only one adsorbate molecule to make a homogenous monolayer on the adsorbent. The linear equation of Langmuir isotherm is expressed as **(Ho, Porter, & McKay, 2002)**:

$$\frac{C_{equ}}{q_{equ}} = \frac{1}{k_l q_{max}} + \frac{C_{equ}}{q_{max}} \quad (5)$$

Where q_{equ} (mg/g) and C_{equ} (mg/g) represent the adsorption at equilibrium and adsorbate concentration respectively, q_{max} (mg/g) is the highest adsorption capability, while k_l (L mg/g) is the energy of adsorption. **Figure 8(a)** and **Table 2** show that Langmuir isotherm relates significantly better with the experimental values of adsorption for Cu (II) ions.

In contrast, Freundlich isotherm states that there are unlimited adsorption sites available and a heterogeneous layer of adsorbate will form on the adsorbent with non-uniform distribution of adsorption heat. The Freundlich equation can be written as **(Covelo, Vega, & Andrade, 2007)**:

$$q_{equ} = k_f C_{equ}^{\frac{1}{n}} \tag{6}$$

Where q_{equ} (mg/g) and C_{equ} (mg/g) are the adsorptions at equilibrium and adsorbate concentration respectively, while k_f (L mg^{-1}) is a unit capability coefficient and n shows the degree of heterogeneity in the adsorption system. The greater the value of n, the more heterogeneous system is **(Moussavi & Khosravi, 2010)**. In **Table 2,** n values greater than 1 designates heterogeneous adsorption. As shown in **Figure 8(b)** and **Table 2** the Freundlich model did not fit well with the experimental data of Cu (II) ions adsorption with lower R^2 values as compared to the Langmuir model. The result confirms CHPLLA nanofibres structure and composition.

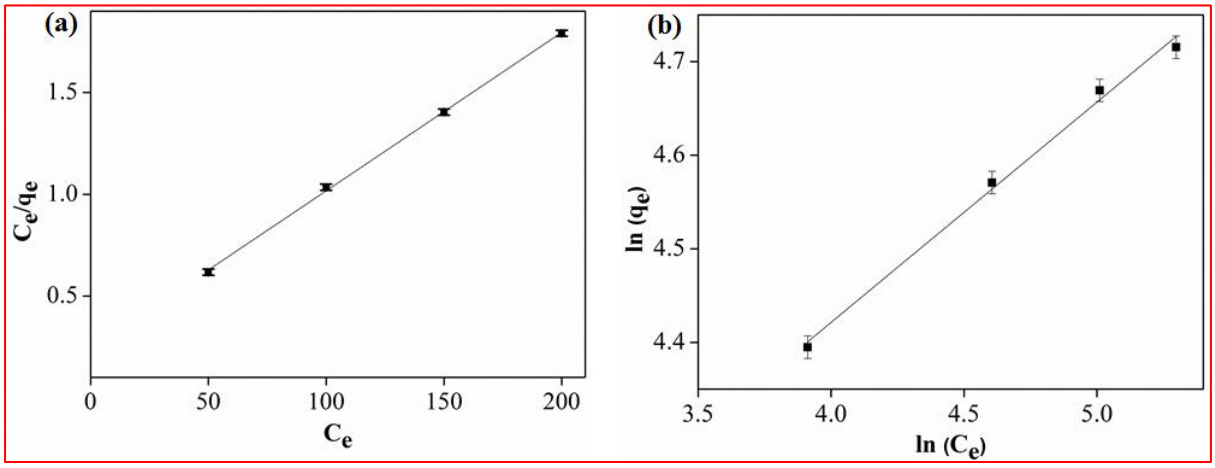

Figure 8. (a): Langmuir adsorption isotherm, (b): Freundlich adsorption isotherm.

Table 2 Parameters of Langmuir and Freundlich isotherm

Metal ion	Freundlich constants				Langmuir constants			
	k_f (L mg^{-1})	n	R^2	SD	k_l (L mg^{-1})	q_{max} (mg g^{-1})	SD	R^2
Cu (II)	3.47	4.24	0.994	±0.012	1.72	128.53	±0.015	> 0.999

3.10. Thermodynamic parameters

The thermodynamic parameters such as Gibbs free energy (ΔG°), enthalpy change (ΔH°) and entropy change (ΔS°) were calculated by thermodynamic equations (7), (8) and (9) **(Li, Zhang, Li, Wang, & Ali, 2016)**:

$$\Delta G° = \Delta H° - T\Delta S° \tag{7}$$

$$k_l = \frac{q_{equ}}{C_{equ}} \tag{8}$$

$$\ln k_l = \frac{\Delta S°}{G} - \frac{\Delta H°}{RT} \tag{9}$$

Where k_l is a constant, q_{equ} is the adsorption capacity (mg/g) at equilibrium, C_{equ} is the metal ion concentration at equilibrium, G is the ideal gas constant (8.314 J/mol/k) and T is the absolute temperature (K). Values of ΔH and ΔS were calculated from the slope and intercept by the linear plot of $\ln k_l$ and the inverse of temperature (1/T) as illustrated in **Figure S4**.

The obtained thermodynamic factors are displayed in **Table S3**. The negative values of ΔH and ΔS indicated a decrease in randomness and exothermic nature of the adsorption process. Therefore, increasing the solution temperature will decrease the binding potential at equilibrium. The negative values of ΔG indicate that the adsorption process was spontaneous in the temperature range studied **(Li et al., 2016)**.

4. Mechanism of chitosan for the removal of Cu ions

Potentiometry is considered to be the fundamental method to describe the complex formation of chitosan with metals by studying acid-base reactions and metal-ligand interactions. The acid accepts a pair of the electron (metal) from the base (chitosan) and forms a covalent bond with the metallic ions. There is only one site available in chitosan monomeric unit (amine groups) which initiates the covalent bonds with metallic ions **(Rhazi, Desbrieres, Tolaimate, Rinaudo, Vottero, Alagui, et al., 2002)**.

During the adsorption process of Cu (II) ions by chitosan, pH of solution plays a notable role **(Rhazi, Desbrieres, Tolaimate, Rinaudo, Vottero, & Alagui, 2002)**. When the pH of a solution is less than 5.30 there is no or very small complex formed between copper Cu (II) ions and chitosan. When pH is greater than 5.30, amino groups made a covalent bond with copper ions and formed $[Cu(\text{-}NH_2)]^{2+}$ complex as shown in **Figure S5** and in the equation (10) and (11):

$$\text{Cu (II)} + \text{-}NH_3^+ + H_2O \rightleftharpoons [Cu(\text{-}NH_2)]^{2+} + H_3O^+ \quad (10)$$

$$\text{Cu (II)} + \text{-}NH_2 \rightleftharpoons [Cu(\text{-}NH_2)]^{2+} \quad (11)$$

Another type of complex was also investigated when pH goes above 5.80 where another amino group is incorporated $[Cu(\text{-}NH_2)_2]^{2+}$as shown in **Figure S5** and in the equations (12) and (13):

$$[Cu(\text{-}NH_2)]^{2+} + \text{-}NH_3^+ + H_2O \rightleftharpoons [Cu(\text{-}NH_2)_2]^{2+} + H_3O^+ \quad (12)$$

$$[Cu(\text{-}NH_2)]^{2+} + \text{-}NH_2 \rightleftharpoons [Cu(\text{-}NH_2)_2]^{2+} \quad (13)$$

This complex is stable up to pH 7.7; beyond this pH, copper hydroxides will precipitate and the procedure will become difficult to study.

5. Conclusion

Chitosan modified porous PLLA nanofibers were fabricated and used as an adsorbent for the elimination of Cu (II) ions from aqueous solution. The adsorption efficiency of this membrane was assessed by varying chitosan concentration, pH, initial metal ion concentration, contact time and temperature. The adsorption capability for copper elevated with increasing contact time and reached equilibrium after 10 minutes. The kinetic studies show that Cu (II) ions adsorption adheres to the second-order kinetics. The highest adsorption ability (128.53 mg/g) was obtained at pH 7 and experimental data of adsorption process suited to a greater degree with Langmuir adsorption isotherm. The adsorption efficiency raised at larger copper ion amounts while at elevated temperature the adsorption capacity of the adsorbent was decreased. Thermodynamic analysis proved that the

adsorption system was exoergic and automatic naturally with negative figures of enthalpy of reaction (ΔH°) and Gibbs free energy (ΔG°). Furthermore, the highest adsorption capability obtained for Cu (II) ions was greater than the figures recorded in previous researches on chitosan-coated adsorbents endorsing that porous supporting material provide more surface area to increase the opportunity of aminic and hydroxide groups of chitosan to bind copper ions. Thus, chitosan modified porous PLLA nanofibrous membrane can be expressed as a green adsorbent for purification of aqueous solutions containing metal ions such as copper.

6. Acknowledgements

We acknowledge the support of the Electron Microscopy Center in The University of Manchester. The project was supported by The Chinese University of Hong Kong and The University of Manchester joint research fund. Finally, the authors thank to Corbion (The Netherlands) company for their supply of PLLA material.

References

Acosta, R. I., Rodríguez, X., Gutiérrez, C., & Moctezuma, M. D. G. (2004). Biosorption of chromium (VI) from aqueous solutions onto fungal biomass. *Bioinorganic Chemistry and Applications, 2*(1-2), 1-7.

Aklil, A., Mouflih, M., & Sebti, S. (2004). Removal of heavy metal ions from water by using calcined phosphate as a new adsorbent. *Journal of Hazardous Materials, 112*(3), 183-190. doi:https://doi.org/10.1016/j.jhazmat.2004.05.018

Aksu, Z., & Kutsal, T. (1991). A bioseparation process for removing lead(II) ions from waste water by using C. vulgaris. *Journal of Chemical Technology & Biotechnology, 52*(1), 109-118. doi:10.1002/jctb.280520108

Barakat, M. A. (2011). New trends in removing heavy metals from industrial wastewater. *Arabian Journal of Chemistry, 4*(4), 361-377. doi:10.1016/j.arabjc.2010.07.019

Barakat, M. A., Chen, Y. T., & Huang, C. P. (2004). Removal of toxic cyanide and Cu(II) Ions from water by illuminated TiO2 catalyst. *Applied Catalysis B: Environmental, 53*(1), 13-20. doi:https://doi.org/10.1016/j.apcatb.2004.05.003

Bassi, R., Prasher, S. O., & Simpson, B. K. (2000). Removal of Selected Metal Ions from Aqueous Solutions Using Chitosan Flakes. *Separation Science and Technology, 35*(4), 547-560. doi:10.1081/SS-100100175

Bhardwaj, N., & Kundu, S. C. (2010). Electrospinning: a fascinating fiber fabrication technique. *Biotechnol Adv, 28*(3), 325-347. doi:10.1016/j.biotechadv.2010.01.004

Bhatt, R., Sreedhar, B., & Padmaja, P. (2017). Chitosan supramolecularly cross linked with trimesic acid - Facile synthesis, characterization and evaluation of adsorption potential for chromium(VI). *Int J Biol Macromol, 104*(Pt A), 1254-1266. doi:10.1016/j.ijbiomac.2017.06.067

Boddu, V. M., Abburi, K., Talbott, J. L., Smith, E. D., & Haasch, R. (2008). Removal of arsenic (III) and arsenic (V) from aqueous medium using chitosan-coated biosorbent. *Water research, 42*(3), 633-642.

Chen, A. H., Liu, S. C., Chen, C. Y., & Chen, C. Y. (2008). Comparative adsorption of Cu(II), Zn(II), and Pb(II) ions in aqueous solution on the crosslinked chitosan with epichlorohydrin. *J Hazard Mater, 154*(1-3), 184-191. doi:10.1016/j.jhazmat.2007.10.009

Chen, A. H., Yang, C. Y., Chen, C. Y., Chen, C. Y., & Chen, C. W. (2009). The chemically crosslinked metal-complexed chitosans for comparative adsorptions of Cu(II), Zn(II), Ni(II) and Pb(II) ions in aqueous medium. *J Hazard Mater, 163*(2-3), 1068-1075. doi:10.1016/j.jhazmat.2008.07.073

Chiou, M. S., & Li, H. Y. (2003). Adsorption behavior of reactive dye in aqueous solution on chemical cross-linked chitosan beads. *Chemosphere, 50*(8), 1095-1105. doi:https://doi.org/10.1016/S0045-6535(02)00636-7

Cooper, A., Oldinski, R., Ma, H., Bryers, J. D., & Zhang, M. (2013). Chitosan-based nanofibrous membranes for antibacterial filter applications. *Carbohydrate Polymers, 92*(1), 254-259. doi:https://doi.org/10.1016/j.carbpol.2012.08.114

Correlo, V. M., Boesel, L. F., Bhattacharya, M., Mano, J. F., Neves, N. M., & Reis, R. L. (2005). Properties of melt processed chitosan and aliphatic polyester blends. *Materials Science and Engineering: A, 403*(1), 57-68. doi:https://doi.org/10.1016/j.msea.2005.04.055

Covelo, E. F., Vega, F. A., & Andrade, M. L. (2007). Simultaneous sorption and desorption of Cd, Cr, Cu, Ni, Pb, and Zn in acid soils: I. Selectivity sequences. *Journal of Hazardous Materials, 147*(3), 852-861. doi:https://doi.org/10.1016/j.jhazmat.2007.01.123

Dorati, R., Pisani, S., Maffeis, G., Conti, B., Modena, T., Chiesa, E., . . . Genta, I. (2018). Study on hydrophilicity and degradability of chitosan/polylactide-co-polycaprolactone nanofibre blend electrospun membrane. *Carbohydrate Polymers, 199*, 150-160. doi:https://doi.org/10.1016/j.carbpol.2018.06.050

Dubey, S. P., & Gopal, K. (2007). Adsorption of chromium(VI) on low cost adsorbents derived from agricultural waste material: A comparative study. *Journal of Hazardous Materials, 145*(3), 465-470. doi:https://doi.org/10.1016/j.jhazmat.2006.11.041

Ferrero, F., Tonetti, C., & Periolatto, M. (2014). Adsorption of chromate and cupric ions onto chitosan-coated cotton gauze. *Carbohydr Polym, 110*, 367-373. doi:10.1016/j.carbpol.2014.04.016

Habiba, U., Siddique, T. A., Joo, T. C., Salleh, A., Ang, B. C., & Afifi, A. M. (2017). Synthesis of chitosan/polyvinyl alcohol/zeolite composite for removal of methyl orange, Congo red and chromium(VI) by flocculation/adsorption. *Carbohydr Polym, 157*, 1568-1576. doi:10.1016/j.carbpol.2016.11.037

Habiba, U., Siddique, T. A., Talebian, S., Lee, J. J. L., Salleh, A., Ang, B. C., & Afifi, A. M. (2017). Effect of deacetylation on property of electrospun chitosan/PVA nanofibrous membrane and removal of methyl orange, Fe(III) and Cr(VI) ions. *Carbohydr Polym, 177*, 32-39. doi:10.1016/j.carbpol.2017.08.115

Ho, Y. S., Porter, J. F., & McKay, G. (2002). Equilibrium Isotherm Studies for the Sorption of Divalent Metal Ions onto Peat: Copper, Nickel and Lead Single Component Systems. *Water, Air, and Soil Pollution, 141*(1), 1-33. doi:10.1023/A:1021304828010

Huang, Z.-M., Zhang, Y. Z., Kotaki, M., & Ramakrishna, S. (2003). A review on polymer nanofibers by electrospinning and their applications in nanocomposites. *Composites Science and Technology, 63*(15), 2223-2253. doi:https://doi.org/10.1016/S0266-3538(03)00178-7

Keizer, H. M. K. K. (2001). Adsorption of Cu(II) and Cr(VI) ions by chitosan: Kinetics and equilibrium studies. *Water SA, 27*(1).

Kurniawan, T. A., Chan, G. Y. S., Lo, W.-H., & Babel, S. (2006). Physico–chemical treatment techniques for wastewater laden with heavy metals. *Chemical Engineering Journal, 118*(1-2), 83-98. doi:10.1016/j.cej.2006.01.015

Labidi, A., Salaberria, A. M., Fernandes, S. C. M., Labidi, J., & Abderrabba, M. (2016). Adsorption of copper on chitin-based materials: Kinetic and thermodynamic studies. *Journal of the Taiwan Institute of Chemical Engineers, 65*, 140-148. doi:10.1016/j.jtice.2016.04.030

Lalita, Singh, A. P., & Sharma, R. K. (2017). Synthesis and characterization of graft copolymers of chitosan with NIPAM and binary monomers for removal of Cr(VI), Cu(II) and Fe(II) metal ions from aqueous solutions. *Int J Biol Macromol, 99*, 409-426. doi:10.1016/j.ijbiomac.2017.02.091

Li, M., Zhang, Z., Li, R., Wang, J. J., & Ali, A. (2016). Removal of Pb(II) and Cd(II) ions from aqueous solution by thiosemicarbazide modified chitosan. *Int J Biol Macromol, 86*, 876-884. doi:10.1016/j.ijbiomac.2016.02.027

Liu, X., Tokura, S., Haruki, M., Nishi, N., & Sakairi, N. (2002). *Surface Modification of Nonporous Glass Beads with Chitosan and Their Adsorption Property for Transition Metal Ions* (Vol. 49).

Middleton, J. C., & Tipton, A. J. (2000). Synthetic biodegradable polymers as orthopedic devices. *Biomaterials, 21*(23), 2335-2346. doi:https://doi.org/10.1016/S0142-9612(00)00101-0

Moussavi, G., & Khosravi, R. (2010). Removal of cyanide from wastewater by adsorption onto pistachio hull wastes: Parametric experiments, kinetics and equilibrium analysis. *Journal of Hazardous Materials, 183*(1), 724-730. doi:https://doi.org/10.1016/j.jhazmat.2010.07.086

Mututuvari, T. M., & Tran, C. D. (2014). Synergistic adsorption of heavy metal ions and organic pollutants by supramolecular polysaccharide composite materials from cellulose, chitosan and crown ether. *J Hazard Mater, 264*, 449-459. doi:10.1016/j.jhazmat.2013.11.007

Naga, N., Yoshida, Y., Inui, M., Noguchi, K., & Murase, S. (2011). Crystallization of amorphous poly(lactic acid) induced by organic solvents. *Journal of Applied Polymer Science, 119*(4), 2058-2064. doi:10.1002/app.32890

Nagib, S., Inoue, K., Yamaguchi, T., & Tamaru, T. (1999). Recovery of Ni from a large excess of Al generated from spent hydrodesulfurization catalyst using picolylamine type chelating resin and complexane types of chemically modified chitosan. *Hydrometallurgy, 51*(1), 73-85. doi:https://doi.org/10.1016/S0304-386X(98)00073-5

Neumann, I. A., Flores-Sahagun, T. H. S., & Ribeiro, A. M. (2017). Biodegradable poly (l-lactic acid) (PLLA) and PLLA-3-arm blend membranes: The use of PLLA-3-arm as a plasticizer. *Polymer Testing, 60*, 84-93. doi:https://doi.org/10.1016/j.polymertesting.2017.03.013

Niu, Y., Ying, D., Li, K., Wang, Y., & Jia, J. (2017). Adsorption of heavy-metal ions from aqueous solution onto chitosan-modified polyethylene terephthalate (PET). *Research on Chemical Intermediates, 43*(7), 4213-4225. doi:10.1007/s11164-017-2866-y

Plazinski, W., Rudzinski, W., & Plazinska, A. (2009). Theoretical models of sorption kinetics including a surface reaction mechanism: A review. *Advances in Colloid and Interface Science, 152*(1), 2-13. doi:https://doi.org/10.1016/j.cis.2009.07.009

Premakshi, H. G., Ramesh, K., & Kariduraganavar, M. Y. (2015). Modification of crosslinked chitosan membrane using NaY zeolite for pervaporation separation of water–isopropanol mixtures. *Chemical Engineering Research and Design, 94*, 32-43. doi:https://doi.org/10.1016/j.cherd.2014.11.014

Qu, R., Sun, C., Ma, F., Zhang, Y., Ji, C., Xu, Q., . . . Chen, H. (2009). Removal and recovery of Hg(II) from aqueous solution using chitosan-coated cotton fibers. *J Hazard Mater, 167*(1-3), 717-727. doi:10.1016/j.jhazmat.2009.01.043

Qu, R., Sun, C., Wang, M., Ji, C., Xu, Q., Zhang, Y., . . . Yin, P. (2009). Adsorption of Au(III) from aqueous solution using cotton fiber/chitosan composite adsorbents. *Hydrometallurgy, 100*(1-2), 65-71. doi:10.1016/j.hydromet.2009.10.008

Râpă, M., Miteluţ, A. C., Tănase, E. E., Grosu, E., Popescu, P., Popa, M. E., . . . Vasile, C. (2016). Influence of chitosan on mechanical, thermal, barrier and antimicrobial properties of PLA-biocomposites for food packaging. *Composites Part B: Engineering, 102*, 112-121. doi:https://doi.org/10.1016/j.compositesb.2016.07.016

Razzaz, A., Ghorban, S., Hosayni, L., Irani, M., & Aliabadi, M. (2016). Chitosan nanofibers functionalized by TiO 2 nanoparticles for the removal of heavy metal ions. *Journal of the Taiwan Institute of Chemical Engineers, 58*, 333-343. doi:10.1016/j.jtice.2015.06.003

Repo, E., Warchoł, J. K., Bhatnagar, A., & Sillanpää, M. (2011). Heavy metals adsorption by novel EDTA-modified chitosan–silica hybrid materials. *Journal of Colloid and Interface Science, 358*(1), 261-267. doi:https://doi.org/10.1016/j.jcis.2011.02.059

Rhazi, M., Desbrieres, J., Tolaimate, A., Rinaudo, M., Vottero, P., & Alagui, A. (2002). Contribution to the study of the complexation of copper by chitosan and oligomers. *Polymer, 43*(4), 1267-1276.

Rhazi, M., Desbrieres, J., Tolaimate, A., Rinaudo, M., Vottero, P., Alagui, A., & El Meray, M. (2002). Influence of the nature of the metal ions on the complexation with chitosan.: Application to the treatment of liquid waste. *European Polymer Journal, 38*(8), 1523-1530.

Salehi, E., Daraei, P., & Arabi Shamsabadi, A. (2016). A review on chitosan-based adsorptive membranes. *Carbohydr Polym, 152*, 419-432. doi:10.1016/j.carbpol.2016.07.033

Seo, S.-J., Kim, J.-J., Kim, J.-H., Lee, J.-Y., Shin, U. S., Lee, E.-J., & Kim, H.-W. (2014). Enhanced mechanical properties and bone bioactivity of chitosan/silica membrane by functionalized-carbon nanotube incorporation. *Composites Science and Technology, 96*, 31-37. doi:https://doi.org/10.1016/j.compscitech.2014.03.004

Shen, C., Wang, Y., Xu, J., & Luo, G. (2013). Chitosan supported on porous glass beads as a new green adsorbent for heavy metal recovery. *Chemical Engineering Journal, 229*, 217-224. doi:10.1016/j.cej.2013.06.003

Tirtom, V. N., Dinçer, A., Becerik, S., Aydemir, T., & Çelik, A. (2012). Comparative adsorption of Ni(II) and Cd(II) ions on epichlorohydrin crosslinked chitosan–clay composite beads in aqueous solution. *Chemical Engineering Journal, 197*, 379-386. doi:10.1016/j.cej.2012.05.059

Unit, S. C. (2013). ***Science for Environment Policy In-depth Report: Soil Contamination: Impacts on Human Health*** Retrieved from http://ec.europa.eu/science-environment-policy

Wan, M.-W., Kan, C.-C., Rogel, B. D., & Dalida, M. L. P. (2010). Adsorption of copper (II) and lead (II) ions from aqueous solution on chitosan-coated sand. *Carbohydrate Polymers, 80*(3), 891-899. doi:10.1016/j.carbpol.2009.12.048

Wan, M.-W., Petrisor, I. G., Lai, H.-T., Kim, D., & Yen, T. F. (2004). Copper adsorption through chitosan immobilized on sand to demonstrate the feasibility for in situ soil decontamination. *Carbohydrate Polymers, 55*(3), 249-254. doi:https://doi.org/10.1016/j.carbpol.2003.09.009

Wang, Y., Pitto-Barry, A., Habtemariam, A., Romero-Canelon, I., Sadler, P. J., & Barry, N. P. E. (2016). Nanoparticles of chitosan conjugated to organo-ruthenium complexes. *Inorganic Chemistry Frontiers, 3*(8), 1058-1064. doi:10.1039/c6qi00115g

Ying W, H. W., Aixi Y and Dijiang W. (2006). Bidegradeable Polylactide/Chitosan Blend Membranes *Biomacromolecules, 7*, 1362-1372.

Zhang, G., Qu, R., Sun, C., Ji, C., Chen, H., Wang, C., & Niu, Y. (2008). Adsorption for metal ions of chitosan coated cotton fiber. *Journal of Applied Polymer Science, 110*(4), 2321-2327. doi:10.1002/app.27515

Zhao, F., Repo, E., Yin, D., & Sillanpaa, M. E. (2013). Adsorption of Cd(II) and Pb(II) by a novel EGTA-modified chitosan material: kinetics and isotherms. *J Colloid Interface Sci, 409*, 174-182. doi:10.1016/j.jcis.2013.07.062